

The phase diagram of the Hubbard model by Variational Auxiliary Field quantum Monte Carlo

Sandro Sorella

*SISSA – International School for Advanced Studies, Via Bonomea 265, 34136 Trieste, Italy; and
Computational Materials Science Research Team, RIKEN Center for Computational Science (R-CCS), Kobe, Hyogo 650-0047, Japan **
(Dated: January 19, 2021)

A systematically improvable variational wave function is proposed for the numerical solution of strongly correlated systems, such as the celebrated Hubbard model. With a stochastic optimization method, based on recent advances in variational Monte Carlo, it is possible to achieve unbiased results in the thermodynamic limit with simple and stable low order polynomial extrapolations to zero temperature. This is achieved much before the so called sign problem gets prohibitive. The convergence to the thermodynamic limit is indeed shown to be possible already for relatively small square lattices with linear dimension $L \simeq 16$, thanks to appropriate averages over several twisted boundary conditions. Results for the phase diagram of the Hubbard model at $U/t = 8$ are reported. As a function of the doping from the half-filled Mott insulating state, several fractional dopings $\delta = 1/8, 1/7, 1/6$ are identified where stripes of length $\xi = \frac{1}{\delta}$ have insulating character. Then phase separation is found to connect these antiferromagnetic phases together with the half filled commensurate one. Moreover, the d-wave uniform state, though very close to the ground state energy, is clearly stable only in the large doping region $> 19\%$.

I. INTRODUCTION

The accurate numerical solution of the Schrödinger equation, namely determining the ground state of a many-body Hamiltonian H , remains the most challenging unsolved problem since the Dirac's formulation in 1931. Historically, important progress, as well as too optimistic promises, occurs periodically at least twice a decade, starting from quantum computers, the Density Functional Theory Kohn-Sham formulation[1], the Density Matrix Renormalization Group (DMRG)[2, 3] and its translation within the tensor network quantum information language[4–6], wrong claims[7–9] about the solution of the sign problem in Quantum Monte Carlo (QMC), systematically improvable wave functions (WFs) based on machine learning assumptions[10, 11], just to mention a few of them.

Apparently, this enormous effort has not been fully satisfactory, at present, for the solution of the most highly debated model in condensed matter, namely the Hubbard model in spatial dimension $D > 1$. For instance, in the last decade, the remarkable growth of tensor network techniques applied to many body physics, has essentially shown that it is possible to define variational WF's ψ that are systematically improvable and depend on a number of variational parameters, growing at most polynomially with the number N of electrons. However, even if it is possible to compute $E = \frac{\langle \psi | H | \psi \rangle}{\langle \psi | \psi \rangle}$ in polynomial time (and this is also not obvious) the problem is always mapped to a complex one: the search for the absolute energy minimum of a function defined by several parameters. Even if this number is polynomial in N , the problem is well known to be hard, namely exponential in N [12]. Thus, until now, all variational methods, and also the one presented in this work are always hard, the feasibility of each, depends only on the moderate speed of the exponential growth in the computational cost and whether or not it is possible to solve a model

with this cost.

Analogously, a considerable impact has recently achieved a new variational WF[10], dubbed restricted Boltzmann machine, inspired by machine learning methodologies. Also within this technique, until now, no much progress for the complete solution of the Hubbard model has been made. So far, there exist only negative statements about d-wave superconductivity or the realization of a striped phase for the particular doping $\delta = 1/8$ [13].

The physical picture is instead more clear for the strong coupling limit of the Hubbard model, the so called t-J model. Several years ago this model has been studied[14] with an almost standard variational Monte Carlo method (VMC) that simply relies on the variational principle: the best wave function ansatz, defined by a set of variational parameters, is the one that minimizes the expectation value of the Hamiltonian studied. At that time, soon after the discovery of high temperature superconductivity, it was reported that superconductivity did not need electron-phonon interaction but the driving force was rather the superexchange spin interaction J . The approach and especially the claim was highly debated and remained controversial even when, several years later, just by tensor network P. Corboz et al., obtained, probably without noticing it, almost the same value[15] of the off-diagonal d -wave superconducting long range order, with also some claim about the existence of stripes in the low doping region.

Despite this success, in recent years, the general believe, that the standard VMC is a biased and almost obsolete technique, is becoming more and more popular in the field of strongly correlated systems. On the other hand one has to acknowledge the important progress made by all these recent variational methods: the realization in a way or another of a systematically improvable ansatz, that, in the standard VMC[16] is not available yet.

Here, the square lattice Hubbard model $H = K_\mu + V$ is studied, where $K_\mu = \sum_{k,\sigma} c_{k,\sigma}^\dagger c_{k,\sigma} (-2t(\cos k_x + \cos k_y) - \mu)$ is the kinetic energy, defined here by the hopping t (set to one in the rest of this work) and the chemical potential μ and $V = U \sum_i n_{\uparrow,i} n_{\downarrow,i}$ is the total number of doubly occupied sites

* sorella@sissa.it

operator scaled by the coupling U of the model, where standard second quantization notations are assumed. We introduce the following ansatz[17–19], also inspired by similar wave functions quite popular in quantum computation[20, 21]:

$$|\psi_\tau\rangle = \exp\left[-\frac{\tau}{2}(H_{MF}(\alpha) + V)\right]|\psi_{MF}\rangle \quad (1)$$

defined by a mean field (MF) Hamiltonian $H_{MF}(\alpha)$ depending on a set $\alpha_1, \alpha_2, \dots, \alpha_p$ of variational parameters indicated here by the vector α . With no loss of generality, H_{MF} is assumed to be a generic operator quadratic in the fermion ones c, c^\dagger and including for instance also a d-wave BCS pairing field, and such that $H_{MF} = K_\mu$ for a particular choice of $\alpha = \alpha_0$ (e.g. $\alpha_0 = 0$). Further p variational parameters, α' define the MF wavefunction $|\psi_{MF}\rangle$ that is assumed to be the ground state of H_{MF} for a *different* set of variational parameters α' . We anticipate that in this variational formulation of the auxiliary field quantum Monte Carlo (VAFQMC) τ play a role of an effective inverse temperature that is kept fixed during the minimization of the energy expectation value corresponding to $|\psi_\tau\rangle$. The main feature of this ansatz is that a mean-field Hamiltonian $H_{MF}(\alpha)$ appears also in the projection. This is particularly important to improve the convergence in τ , by systematically correcting the starting mean-field ansatz $|\psi_{MF}\rangle$ with an appropriate many-body projection operator $\exp\left[-\frac{\tau}{2}(H_{MF}(\alpha) + V)\right]$.

The optimization techniques known in standard variational Monte Carlo[22] and machine learning[23] will be generalized here to the auxiliary field QMC. Before that, it is worth to emphasize simple but important properties of this ansatz

1. It is systematically improvable. In order to realize this property, it is enough to take, $\alpha = \alpha_0$ and let $\tau \rightarrow \infty$ for whatsoever mean field ψ_{MF} non orthogonal to the ground state. In this limit $\psi_\tau \simeq \exp(-\frac{\tau}{2}H)|\psi_{MF}\rangle$ is obviously converging to the exact ground state.
2. It is size extensive. As discussed in Ref.16 the WF is defined directly in terms of an exponential of an extensive operator, hence the statement. In practice this means that, at a given τ , approximately the same accuracy for intensive quantities is expected, e.g. the energy per site or bulk correlation functions.
3. For finite size the convergence is exponential in τ due to the finite size gap between the ground state manifold (which may be also degenerate) and the first excitation with non zero energy gap. However in the thermodynamic limit this gap is probably always vanishing in this model, even for the half filled insulator, where gapless spin-wave excitations are expected due to the occurrence of antiferromagnetic order for any $U > 0$ [24]. This situation, as it will be shown in the following, makes the extrapolation to the $\frac{1}{\tau} = 0$ unbiased limit much simpler than the corresponding finite size case, because can be obtained by simple and stable low order polynomial extrapolations in something that can be considered an effective temperature $T_{eff} = 1/\tau$.

The key idea of this work is to converge first the results to the thermodynamic limit with large enough cluster size simulations and appropriate boundary conditions (see later) and then employ simple and very stable extrapolations in the effective temperature T_{eff} , thus achieving, with this simple minded strategy, unbiased results of the model. As it will be shown later this is possible because, after the optimization, the physical properties of our ansatz given in Eq.(1) are indeed already in the very low temperature regime where the extrapolation to $T_{eff} = 0$ is indeed stable and reliable. However it is possible that, as in any optimization technique, it is not possible to identify the correct ψ_{MF} , either because the optimization has been trapped in a spurious local minimum or, more importantly, the right type of order has not been included (e.g. allowing only for homogeneous phases, excluding for instance the possibility to determine a stripe in the ground state). Also in such case the extrapolation to the $T_{eff} \rightarrow 0$ limit can be useful because one can assume that the correct order establishes in ψ_τ for $T_{eff} < T_c$ (where usually simulation are not possible due to sign problem) but everything is smooth and analytic for $T_{eff} > T_c$ so that extrapolation to $T_{eff} \rightarrow 0$, when reliable, allows the unbiased estimation of the lowest possible energy state of a given phase described by the order parameter considered in the chosen mean field ansatz.

It is well established[25] that, when a standard type of order that breaks a continuous symmetry sets in, the corresponding gapless low energy excitations (i.e. typically bosons with a density of states $\rho(\epsilon) \propto \epsilon^{D-1}$) induce $\simeq T^3$ ($\simeq T^2$) energy corrections (i.e. $\Delta E \propto \int_0^T \epsilon \rho(\epsilon) \simeq T^{D+1}$) in the limit $T \rightarrow 0$ for 2D (quasi 1D system like a finite number of infinite legs), and indeed it turns out that the fit $E(T_{eff}) = E(0) + aT_{eff}^{D+1} + bT_{eff}^{D+2}$ is very good for the systems studied here, because the available T_{eff} are clearly small enough to reach the correct asymptotic behavior, thanks to the efficiency of the present projection technique and the optimal initial wavefunction ψ_{MF} used (see supplementary information for a test of the approach in the 2D half-filled case where exact ground state results are available).

Given the above arguments particularly useful boundary conditions are adopted such that the convergence to the thermodynamic limit at fixed τ is as fast as possible. To this purpose twisted averaged boundary conditions TABC[26, 27] are used with opposite twists for opposite spin electrons and they are averaged on a mesh of 16×16 twists in the reciprocal BZ, large enough to have converged results within statistical errors. When H_{MF} conserves the number of particles the so called TABC[26] is used, namely for each twist the number of particles is not changed, whereas when a BCS pairing is present, the grand canonical ensemble is adopted as discussed in Ref.28. The use of opposite twists for opposite spin electrons is particularly important in this case because it allows the conservation of the translation symmetry in the BCS mean field Hamiltonian, at least in a simple way.

Before explaining how to optimize the variational parameters it is useful to appreciate in Fig. (1) the fast and smooth convergence of the grand canonical Gibbs energy $\Omega = H - \mu N$ in the thermodynamic limit as a function of the number of sites

$N_s = L \times L$ for a value of the chemical potential corresponding to doping $\delta \approx 1/8$.

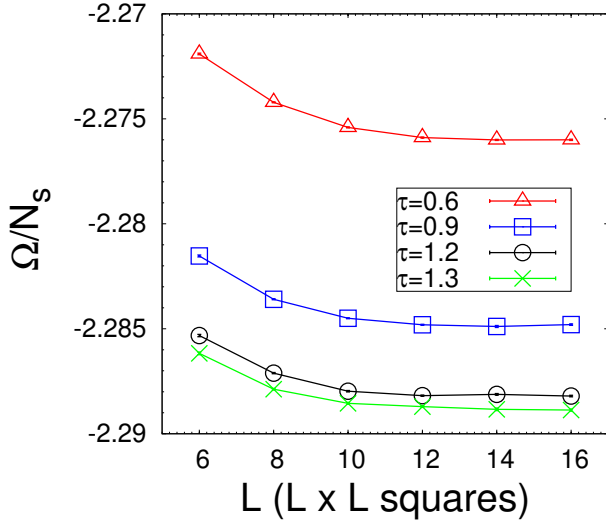


FIG. 1. Gran canonical Gibbs energy per site Ω/N_s as a function of cluster size for different values of the projection time τ for $\mu = 1.75t$ and $U/t = 8$

The other important ingredient for an efficient implementation of Eq. (1) is the use of a particularly suited Trotter decomposition for the corresponding propagator:

$$\exp\left[-\frac{\tau}{2}(H_{MF}(\alpha) + V)\right] = \left\{ \prod_{i=1}^n \exp[-t_i H_{MF}(\alpha)] \exp[-h_i V] \right\} \times \exp[-t_{n+1} H_{MF}(\alpha)] \quad (2)$$

where in principle h_i and t_i can be independently optimized to minimize the Trotter error, as proposed in a recent work[20]. Henceforth it is assumed that the operators in Eq. (2) are ordered from left to right according to increasing values of the integer i . In this work τ is kept fixed, and therefore the following constraint is imposed:

$$\sum_{i=1}^n h_i = \frac{\tau}{2}. \quad (3)$$

Moreover, in order to minimize the number of variational parameters and the number n , the following parametrization is adopted:

$$h_i = \Delta\tau\gamma^{i-1} \quad (4)$$

$$t_i = \frac{h_i + h_{i-1}}{2} \text{ for } i = 1, 2, \dots, n \quad (5)$$

with $h_0 = 0$ and $\gamma > 1$ chosen in a way to satisfy the constraint in Eq. (3). This expression is based on the conventional small $\Delta\tau$ symmetric Trotter decomposition $\exp[-\Delta\tau(H_{MF}(\alpha) + V)] = \exp[-\frac{\Delta\tau}{2}H_{MF}(\alpha)] \exp[-\Delta\tau V] \exp[-\frac{\Delta\tau}{2}H_{MF}(\alpha)] + O(\Delta\tau^3)$, where a non uniform time step according to Eq. (4) has been

chosen because, for high accuracy, it is important only that the first time step is small and $\gamma \simeq 1$. In this way the efficiency and the number of operators involved is significantly optimized, without using too many variational parameters as in Ref.20. In most cases $\Delta\tau t = 0.025$ and $n = [10\tau]$, otherwise the former is optimized when it is not specified.

II. AUXILIARY FIELD METHOD

Since $H_{MF}(\alpha)$ is a one body operator and ψ_{MF} is a mean-field state (e.g. a Slater determinant) there is no difficulty to apply $\exp[-t_i H_{MF}(\alpha)]$ to ψ_{MF} and taking into account that $\exp[-t_i H_{MF}(\alpha)] \psi_{MF}$ remains a mean field state, this operation can be also performed iteratively.

The application of $\exp(-h_i V)$ is instead more complicated and can nevertheless be implemented by using the auxiliary field technique. To this purpose the following exact relation is used:

$$\exp(-h_i V) = 2^{-N_s} \exp(-U h_i N/2) \sum_{\sigma_{j,i}=\pm 1} \exp(\lambda_i \sum_j \sigma_{ji} m_j) \quad (6)$$

where $m_j = n_{j,\uparrow} - n_{j,\downarrow}$, N is the total number of particles operator, $\cosh \lambda_i = \exp(U h_i)$ and the Ising variables $\sigma_{ji} = \pm 1$ for each site j of the lattice, having N_s sites in a $L_x \times L_y$ rectangular lattice. Notice that the factor $\exp(-U h_i N/2)$ represents only an irrelevant change of the chemical potential in $H_{MF}(\alpha)$. Therefore this term is omitted for simplicity here and henceforth.

We get therefore that the expectation value of the Hamiltonian H for the wave function in Eq.(1) is given by:

$$E_n = \frac{\langle \psi_n | H | \psi_n \rangle}{\langle \psi_n | \psi_n \rangle} \quad (7)$$

$$= \frac{\sum_{\sigma \sigma'} \langle \psi_{MF} | U_n^\dagger(\sigma') H U_n(\sigma) | \psi_{MF} \rangle}{\sum_{\sigma \sigma'} \langle \psi_{MF} | U_n^\dagger(\sigma') U_n(\sigma) | \psi_{MF} \rangle} \quad (8)$$

where σ indicates the $N_s \times n$ dimensional vector with components σ_{ji} , and:

$$U_n(\sigma) = \exp(-H_{MF}(\alpha)t_1) \exp(\lambda_1 \sum_j \sigma_{j,1} m_j) \dots \exp(-H_{MF}(\alpha)t_n) \exp(\lambda_n \sum_j \sigma_{j,n} m_j) \exp(-H_{MF}(\alpha)t_{n+1}) \quad (9)$$

E_n can be therefore computed by Monte Carlo, by sampling the Ising fields σ and σ' according to the weight $|W_n(\sigma', \sigma)|$, where:

$$W_n(\sigma', \sigma) = \langle \psi_{MF} | U_n^\dagger(\sigma') U_n(\sigma) | \psi_{MF} \rangle \quad (10)$$

and, quite generally in the complex case, W_n has a non trivial phase that is determined by $S_n(\sigma', \sigma) = \frac{W_n(\sigma', \sigma)}{|W_n(\sigma', \sigma)|}$, a complex number with unit modulus, that plays the role of the QMC sign (often a problem but not in this case) that, as well known, is very important away from the half-filled band condition ($\mu \neq U/2$).

Finally E_n can be computed by :

$$E_n = \frac{\sum_{\sigma\sigma'} |W_n(\sigma', \sigma)| e_n(\sigma', \sigma) S_n(\sigma', \sigma)}{\sum_{\sigma\sigma'} |W_n(\sigma', \sigma)| S_n(\sigma', \sigma)} \quad (11)$$

namely by evaluating the ratio of the means corresponding to two real random variables $\Re[e_n(\sigma', \sigma) S_n(\sigma', \sigma)]$ and $\Re[S_n(\sigma', \sigma)]$ [29] over the configurations generated by Monte Carlo sampling according to the probability $p_n(\sigma', \sigma) = \frac{|W_n(\sigma', \sigma)|}{\sum_{\sigma\sigma'} |W_n(\sigma', \sigma)|}$, using the standard technique described in Ref.16, and:

$$e_n(\sigma', \sigma) = \frac{\langle \Psi_{MF} | U_n^\dagger(\sigma') H U_n(\sigma) | \Psi_{MF} \rangle}{W_n(\sigma', \sigma)} \quad (12)$$

is a sort of local energy, namely an estimate of E_n for a given configuration of the Ising fields σ and σ' . Indeed both $e_n(\sigma', \sigma)$ and $S_n(\sigma', \sigma)$, as well as $W_n(\sigma', \sigma)$ can be computed in $\propto N_s^3 n$ operations because they involve essentially imaginary time propagations of mean-field states under time dependent one body propagators $U_n(\sigma)$ and $U_n(\sigma')$.

The basic ingredient introduced in this work is the possibility to compute energy derivatives of E_n with respect to all the parameters defining the WF, i.e. α and α' , henceforth assumed to be defined by the $2p$ variational parameters $\alpha_1, \alpha_2, \dots, \alpha_{2p}$ and the minimum time step used $\Delta\tau = \alpha_{2p+1}$ at fixed τ , according to Eq.(3). A simple algebra, very similar to the one known for VMC, implies that any energy derivative $\frac{\partial E_n}{\partial \alpha_j}$ with respect to an arbitrary variational parameter α_j , for $j = 1, 2, \dots, 2p + 1$, can be computed by means of corresponding derivatives of two complex functions $\frac{\partial e_n}{\partial \alpha_j}$, $O_j = \frac{\partial \ln(W_n)}{\partial \alpha_j} = \frac{\partial W_n}{\partial \alpha_j} / W_n$ of the local energy and the logarithm of the weight, respectively:

$$\frac{\partial E_n}{\partial \alpha_j} = \frac{\langle \langle \Re \{ S_n \left[\frac{\partial e_n}{\partial \alpha_j} + (e_n - E_n) O_j \right] \} \rangle \rangle}{\langle \langle \Re(S_n) \rangle \rangle} \quad (13)$$

where here and henceforth the symbol $\langle \langle * \rangle \rangle$ indicates the average of the generic random variable $*$ over the probability distribution p_n defined before, and for shorthand notations the dependence on σ and σ' of all the quantities involved is not explicitly shown.

The differentiation of the complex quantities $\ln W_n$ and e_n , required for the $\frac{\partial E_n}{\partial \alpha_j}$ evaluation, at given values of σ and σ' , may appear very cumbersome and involved especially considering that, it is often necessary, as in VMC, to optimize several parameters. This task can be easily achieved in a computational time equal to the one required to compute the complex quantities $\ln(W_n)$ and e_n , remarkably only up to a small prefactor regardless how large is the number of variational parameters involved. This is possible by using Adjoint Algorithmic Differentiation (AAD)[30], a technique that is becoming popular in the field of Machine Learning with another name, i.e. "back propagation", but was certainly known before in applied mathematics[31], and only recently has been appreciated

in physics[32, 33]. Once all energy derivatives $\partial_j E$ are known, the usual scheme adopted in VMC can be applied also here. Variational parameters are changed according to the equation:

$$\delta \alpha = -\text{rate}_{\text{learning}} S^{-1} \frac{\partial E}{\partial \alpha} \quad (14)$$

where $\text{rate}_{\text{learning}}$ is a suitable small constant, determining the speed of convergence to the minimum and S is the so called Fisher-information matrix, given by:

$$S_{ij} = \langle \langle \frac{\partial \log p_n}{\partial \alpha_i} \frac{\partial \log p_n}{\partial \alpha_j} \rangle \rangle = \langle \langle \langle \Re(O_i) \Re(O_j) \rangle \rangle \rangle \quad (15)$$

where the symbol $\langle \langle \langle AB \rangle \rangle \rangle = \langle \langle AB \rangle \rangle - \langle \langle A \rangle \rangle \langle \langle B \rangle \rangle$ indicates here the covariance of two random variables over the probability p_n . We adopt here $\text{rate}_{\text{learning}} \simeq 6$ and the same regularization with $\varepsilon = 0.01$ described in Ref. ([16]) to avoid instabilities in the calculation of the inverse matrix. Typically convergence is reached with a few hundreds iterations and, variational parameters are averaged after convergence for about 50 steps.

III. RESULTS

First VAFQMC is tested at $U/t = 8$ on a finite number L_y of legs with PBC in the y - direction, in order to compare with the the very accurate results determined by DMRG in the $L_x = \infty$ one dimensional thermodynamic limit. As it is seen in Fig. (2) VAFQMC is in perfect agreement with the known results for $L_y \leq 6$ once the $T_{eff}^2 \rightarrow 0$ extrapolation is employed in a relatively small $L_y \times 16$ cluster with 32 twists in the long direction (convergence in the thermodynamic limit has also been verified by comparing with the 4×32 cluster). In this case, at doping $\delta = 1/8$ it has been found that the $\xi = 8$ - length stripe is the most favorable mean-field, that is here parametrized (see supplementary information) by the most general solution (independent of y) with local magnetic antiferromagnetic field $\Delta_{AF}(x) = -\Delta_{AF}(x + \xi)$ (x and y represent here the integer cartesian coordinates of the lattice) and corresponding to a local chemical potential $\mu_x = \mu_{x+\xi}$ and nearest neighbor hoppings $t_x(x) = t_x(x + \xi)$ and $t_y(x) = t_y(x + \xi)$, amounting to a total of $8\xi + 1$ variational parameters in Ψ_τ , that are assumed independent of the twists[28]. The few parameter choice adopted in Ref.34 is used only to initialize our most general $8\xi + 1$ parameters ansatz. For the uniform solution (see supplementary information) antiferromagnetic order is allowed only at half filling while at finite doping a four parameter ansatz is adopted in $H_{MF}(\alpha)$ including nearest and next nearest neighbor hoppings as well as a uniform chemical potential μ_0 and $d_{x^2-y^2}$ pairing.

With this method it is therefore possible to compute the energy in the thermodynamic limit of 8-legs without particular effort as the average (complex-) sign $\langle \langle S_n \rangle \rangle$ is always larger than 0.5 for the simulations reported in this case. It is important to remark that, when the 2D-thermodynamic limit is approached, a small but systematic increase of the energy can

be appreciated, confirming that, in order to determine the correct two dimensional thermodynamic limit, true two dimensional clusters have to be used.

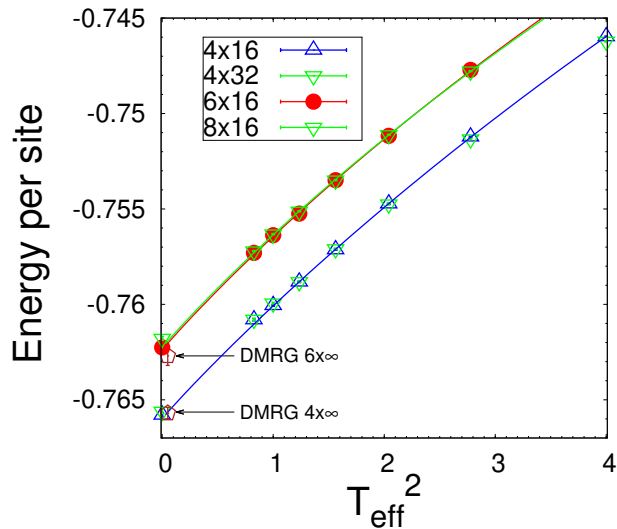


FIG. 2. Energy as a function of the effective temperature $T_{eff} = 1/\tau$ for different number of legs compared with DMRG. Here $\Delta\tau = 0.025$.

That for L_y small the stripe solution can be favored, as correctly found by DMRG, is shown in Fig. 3. At the chemical potential $\mu = 1.825t$, corresponding to $\delta \simeq 1/8$, the gran canonical energy Ω of the stripe solution (computed in the stripe case by $\Omega(\mu) = \min_N \langle H - \mu N \rangle$ with calculation at fixed number of particles and $N \simeq N_s \times 7/8$) is clearly below the one corresponding to the uniform phase by more than $0.003t$ per site. However the situation is much different when

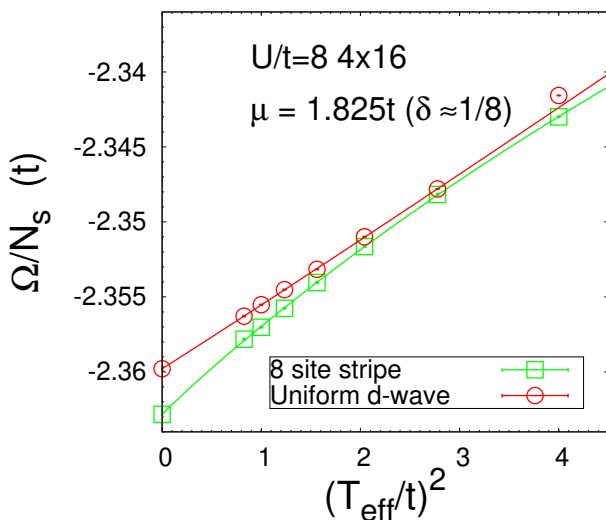


FIG. 3. Gran canonical Gibbs energy per site Ω/N_s at $\mu = 1.825t$ for the stripe solution and the uniform d -wave superconducting one.

the two dimensional thermodynamic limit is required. In all these cases we have optimized $\Delta\tau$ with the choice:

$$n = \text{Max} \{[(\tau U/0.4 - 1)/5], 1\} \quad (16)$$

because the calculations are quite heavy in large clusters, especially considering that it is important to be extremely accurate in the optimization to obtain accurate fits. As for any extrapolation there may be a small systematic error in determining the $T_{eff} \rightarrow 0$ unbiased results. For instance the correction implied by the extrapolation to all the best variational energy values at $\tau t = 1.3$ is $\simeq 0.002t$ per site, and therefore a bias of order $\simeq 0.001t$ may be expected. However, since in all 2D cases we have adopted the same type of extrapolation and used the same range of effective temperatures, it is plausible that extrapolated energy differences should be very accurate, because most of the systematic bias should cancel out in the differences. In this way, in order to compare the stripe with periodicity $\xi = 8$ ($\xi = 7, 6, 5$ will be also reported later) and the uniform d -wave solution, calculations on a 16×16 ($14 \times 14, 12 \times 12, 20 \times 12$) cluster are carried out with 16×16 different twists, where now $\mu = 1.75t$ is chosen to fulfill a doping $\delta \simeq 1/8$. It is clearly seen from the Fig. (4) that, despite for finite τ the stripe solution has lower energy, the extrapolation to $T_{eff} \rightarrow 0$ clearly favors the uniform phase, as it is also seen by the very small energy difference $\simeq 0.001t$ reached at the lowest T_{eff} shown. The reason

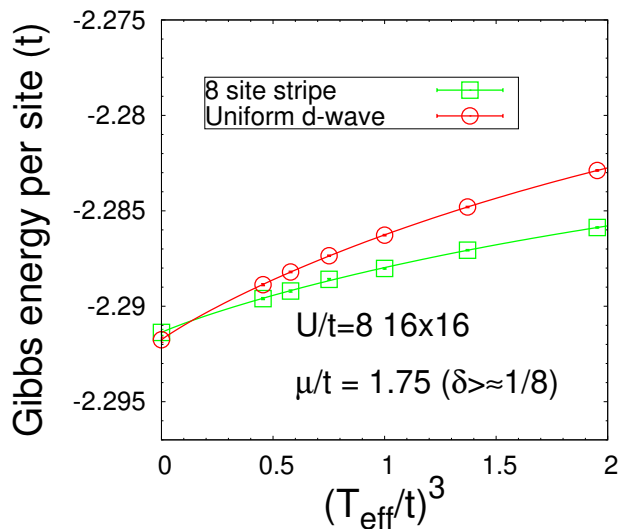


FIG. 4. Gran canonical Gibbs energy per site Ω/N_s at $\mu = 1.75t$ for the stripe solution and the uniform d -wave superconducting one.

why the convergence in T_{eff} is faster for the 8-length stripe case is because the corresponding ground state has a charge gap at $\delta = 1/8$ as opposed to the uniform d -wave state that is gapless in both charge and spin sectors. At fractional doping, a finite gap for the stripe solution has been reported also in Ref.34. The occurrence of a finite gap in this case is easily understood because this incommensurate state is adiabatically connected to the insulator having equally spaced empty (i.e. with no-electrons) vertical lines of sites separating half-filled

antiferromagnetic insulating region. This finite gap is quantitatively estimated here in Fig. (5) because $\mu = -\frac{\partial E_N}{\partial N}$ has a clear jump ($\delta = (1 - N/N_s)$) at $\delta = 1/8$, implying that the charge gap $\Delta_c = \mu_+ - \mu_- \simeq 0.12t$, where μ_+ (μ_-)[35] is the chemical potential computed by increasing (decreasing) the number of particles with respect to the reference one. A table of the charge gap $\mu_+ - \mu_-$, calculated in this way at commensurate dopings is reported in Tab.(I). In this table it is evident that the $\xi = 6$ stripe is particularly stable, having the largest gap. Conversely the $\xi = 5$ one melts down with increasing τ because the doping $1/5$ appears too large to sustain incommensurate antiferromagnetic order.

ξ	μ_-	μ_+	Gap
6	1.5441(40)	1.7589(40)	0.2148(57)
7	1.6645(85)	1.7686(81)	0.104(12)
8	1.6981(58)	1.8128(56)	0.1147(77)

TABLE I. Upper (μ_+) and lower (μ_-) chemical potential for which the hole doping δ acquires a fractional value $\frac{1}{\xi}$, in an insulating phase with finite charge gap (Gap). ξ indicates the length of the stripe as discussed in the text. The numbers in parenthesis represent error bars in the last digits.

At this point it is important to remark why the grand canonical Gibbs energy is very appropriate to study the phase separation instability even when the Hamiltonian commutes with the particle number as the case studied. Once $\Omega(\mu)/N_s$ is given in the thermodynamic limit, the corresponding ground state energy per site is easily found by the Legendre transform $-E(N) = \Omega + \mu \frac{\partial \Omega}{\partial \mu}$ where the number of particles N depends on μ by the relation $N = -\frac{\partial \Omega}{\partial \mu}$. However, when phase separation occurs, not all values of dopings $\delta = 1 - N/N_s$ are possible, and this quantity jumps discontinuously from a smaller δ_- to a larger doping δ_+ when decreasing the chemical potential μ : this represents just a manifestation of phase separation between an hole rich phase at doping δ_+ to an hole poor phase at doping δ_- , as for instance the case discussed in Ref.36 for the phase separation between the half-filled antiferromagnetic insulating phase ($\delta_- = 0$) and the hole rich phase.

In the present phase diagram of the Hubbard model several insulating phases appear at commensurate doping $\frac{1}{\xi}$ and the doping $\delta = 1/\xi$ does not change when $\mu_- \leq \mu \leq \mu_+$ (with μ_+ clearly larger than μ_- as reported in Tab. I), provided the corresponding phase is the one with the minimum Ω/N_s . This is clearly the case for $\xi = 6$ and $\xi = 7$, as shown in Fig. (6) whereas for $\xi = 8$ there is evidence that a metallic stripe is stable as seen for $\mu = 1.85t$ when $\delta > 1/8$ according to Tab. I and a gapless behavior appears in Fig. 5. In summary, consistently with the results of Tab. I and Fig. 6 it is possible to conclude that there exist four doping intervals where phase separation occurs, as reported in Fig. (7).

It is important to remark that the uniform phase has a very good energy, competing with the lowest possible ones. Indeed in Fig. (6) the uniform d -wave phase loses only a tiny energy (always less than $0.001t$ per site) vs the non uniform stripe phases and is also likely to be the stable one for δ very close to $1/8$, i.e. $\mu/t \simeq 1.8$. It is also clear in this picture

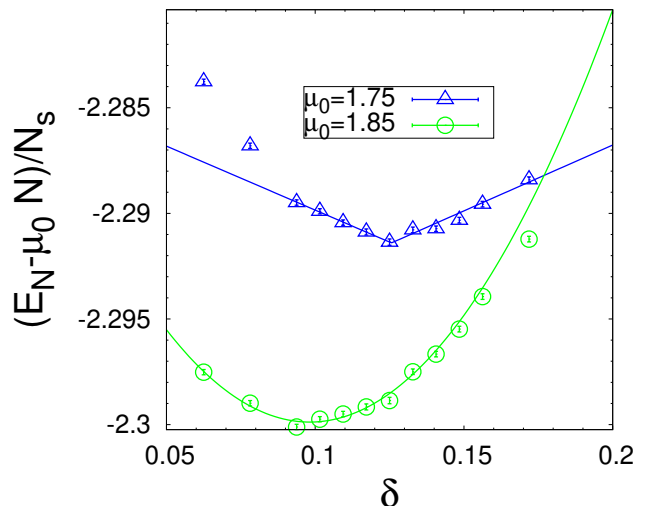


FIG. 5. Total energy (shifted by $-\mu_0 N$ for clarity) per site for the 8-length stripe solution as a function of the doping δ . The results for $\mu_0 = 1.85t$ are shifted upwards by $0.08t$ for clarity.

that phase separation[36] should indeed occur for $\mu > 1.913t$ even if we take into account the small energy gain provided by the incommensurate stripe solutions. This small change is clearly not able to provide a grand canonical Gibbs energy $\Omega/N_s < E_h - \mu$ where $E_h = -0.5244(14)$ is the energy per site of the half filled Hubbard model at $U/t = 8$, estimated with the same type of WF in Eq.(1) with $\tau t \leq 1.3$ energy evaluations. This reference is in good agreement with previous benchmark calculations[37] (see supplementary material). Remarkably, the $\xi = 16$ stripe, within this approach, does

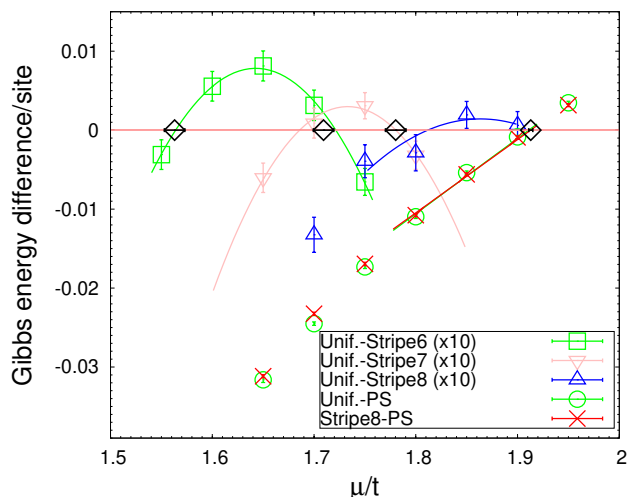


FIG. 6. Difference of Ω/N_s (positive values indicate stable non-uniform phases) between the uniform d -wave phase and the stripe phase, or the phase separated (PS) phase made of an hole rich phase and the half-filled antiferromagnetic phase.

not provide an Gibbs energy Ω/N_s below the above benchmark even around doping $\delta \simeq 1/16$, supporting even more strongly the phase separation for $\delta \leq 8\%$. It is also inter-

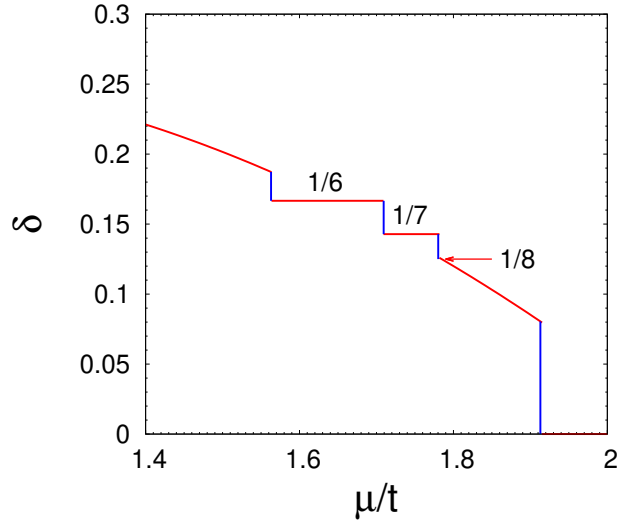


FIG. 7. Hole doping δ as a function of the chemical potential μ . Not all values of δ are allowed, and therefore vertical blue lines indicate phase separation doping regions between the two homogeneous phases corresponding to the interval extreme dopings.

esting that, within our approach, the d -wave superconducting order does not coexist with the stripe solution, contrary to standard variational approach[34], and an interesting metallic stripe (i.e. with $\delta < 1/8$) with no pairing should be the stable phase before phase separation. Moreover the d -wave uniform phase, competing with this stripe phase in the low doping regime $\delta \leq 1/8$, has a vanishingly small order parameter when approaching the phase separation occurring at $\delta = 0.08$, as shown in the inset of Fig. (8). This is consistent with the $\xi = 8$ stripe solution in supporting the existence of a low doping metallic phase just before phase separation.

On the other hand, in order to determine, the upper critical doping δ_c above which a Fermi liquid phase or an exponentially small pairing of the Kohn-Luttinger type exists[38, 39] in Fig.(8) the superconducting $\Delta_{x^2-y^2}$ parameter corresponding to our variational calculation is displayed. It is evident that size effects are negligible and that superconductivity disappears around $\mu/t = 1.4$ (see also inset). The doping δ corresponding to a given chemical potential μ can be determined by the derivative of Ω/N_s in the thermodynamic limit, by the relation $\delta = 1 + \partial_\mu \Omega/N_s$, where (see supplementary information):

$$\Omega/N_s = -0.91529 - 0.90248\mu + 0.17684\mu^2 - 0.06318\mu^3 \quad (17)$$

is a very good interpolation of our $T_{eff} \rightarrow 0$ results of the uniform state for $1.4 \leq \mu \leq 1.95$ with less than 3×10^{-4} error. This implies that superconductivity disappears or is exponentially small at $\delta_c = 0.221(2)$ corresponding to $\mu/t = 1.4$. This is also in good agreement with the direct evaluation of the

pairing correlation (see inset Fig. 8). The final phase diagram is therefore reported in Fig. (9).

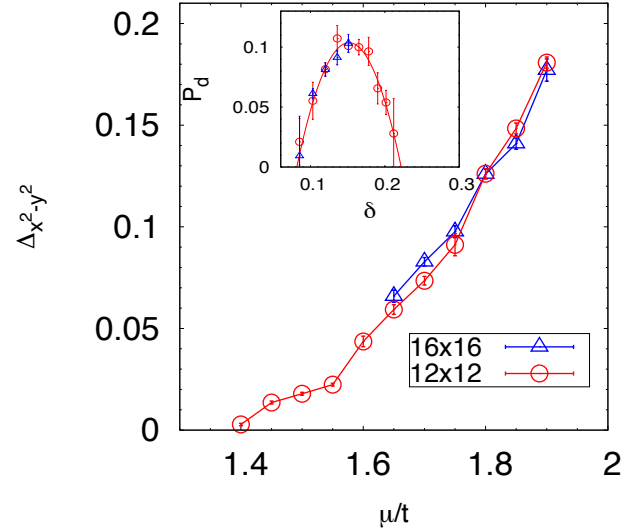


FIG. 8. $\Delta_{x^2-y^2}$ BCS pairing variational parameter in the mean-field Hamiltonian H_{MF} defining our spatially uniform variational ansatz of Eq. (1), as a function of the chemical potential μ for the lowest T_{eff} and largest clusters considered. Inset: value of the corresponding BCS order parameter as a function of the doping δ evaluated with the $T_{eff} \rightarrow 0$ linear extrapolation of the pairing-pairing correlations at distance $L/2$. The error bars include also uncertainty in this extrapolation.

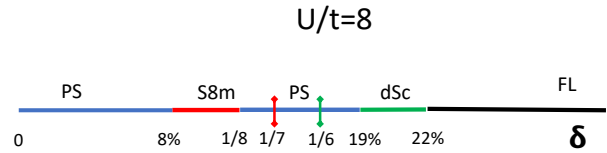


FIG. 9. Phase diagram of the Hubbard model by VAFQMC. Blue lines indicate phase separation regions in between several insulating phases occurring at fractional dopings. S8m indicate a metallic stripe phase with length $\xi = 8$ that has been found to be almost degenerate with a d -wave uniform state. The d -wave superconductivity indeed begins to be clear for $\delta > 1/6$ when phase separation occurs with the corresponding uniform one at $\delta = 19\%$. This phase in turn remains stable (dSc) up to 22%. After this doping a Fermi liquid (FL) metal or an exponentially small pairing[38] is possible. Most of the transitions are obviously first order ones.

IV. CONCLUSIONS

In this work we have introduced a new method VAFQMC that is able to exploit the power of the auxiliary field technique combined with the simplicity and generality of the standard variational quantum Monte Carlo method. We have here combined these two successful approaches to strongly correlated systems, and estimated the phase diagram of the Hubbard model, disentangling the most stable phases at $U/t = 8$, among the plausible ones described by the general mean field ansatz ψ_{MF} . This phase diagram is *in principle exact* as long as the correct order parameters have been used to parametrize ψ_{MF} .

It has been shown that unbiased results in the thermodynamic limit can be obtained by minimizing the energy of a systematically improvable variational wavefunction that is exact for $\tau = \infty$. In the thermodynamic limit a further simplification is possible because the results can be easily extrapolated to the unbiased $T_{eff} = 1/\tau = 0$ case, with low order polynomials in T_{eff} , consistent with the known low temperature scalings. The conventional approach is to attempt exact calculations (usually very hard if not impossible) at finite L and try to extrapolate to $\frac{1}{L} \rightarrow 0$. Here we have shown that it is much simpler and indeed possible to extrapolate with VAFQMC only in the effective temperature $T_{eff} \rightarrow 0$ with calculations essentially converged in $\frac{1}{L} \rightarrow 0$.

The present results are qualitatively consistent with the most accurate previous calculations (standard variational, AFQMC with the constrained path approximation, DMRG in $D > 1$) that stripes should be important in the low doping region of the Hubbard model. However the complete and accurate solution for all dopings sheds lights on the dominant

role of phase separation in 2D strongly correlated systems, that definitively occurs close to half filling. This phenomenon was also reported in previous works[40, 41], only very close to half-filling.

The time is now enough mature to draw some conclusions on the several hypotheses that were born in the '90s to explain high temperature phenomenology with this model. The proximity to a phase separation instability at low doping, confirms once more that the Kivelson and Emery's idea was the key breakthrough[36] of that period.

Several new applications and extensions are possible within VAFQMC, the technique presented in this work. The WF ψ_{τ} can be further generalized to more realistic Hamiltonians, including for instance long range Coulomb interaction or electron-phonon coupling. A simple improvement is to consider also correlated terms beyond U in Eq. (1), as for instance in the strong coupling limit a term proportional to the superexchange J should be expected. The finite effective temperature T_{eff} defined for a variational wavefunction in the thermodynamic limit was the key to obtain unbiased results for this model, a feature that could be possibly generalized to several other computational techniques, from tensor networks to machine learning variational wave functions.

ACKNOWLEDGMENTS

Acknowledgements: I am grateful for very useful discussions with E. Tosatti, G. Carleo, N. Costa, A. Tirelli, F. Becca, L. Capriotti, M. Fabrizio, S. Yunoki and especially A. Parola, who have shared with me the same passion for this model for about thirty years. I acknowledge PRACE for awarding access to Marconi at CINECA Italy, and Riken collaboration for access to HOKUSAI supercomputer in Saitama Japan, as well as financial support from PRIN 2017BZPKSZ.

-
- [1] W. Kohn and L. J. Sham, Phys. Rev. **140**, A1133 (1965).
 - [2] S. R. White, Phys. Rev. Lett. **69**, 2863 (1992).
 - [3] U. Schollwöck, Rev. Mod. Phys. **77**, 259 (2005).
 - [4] R. Orús, Annals of Physics **349**, 117 (2014).
 - [5] F. Verstraete, D. Porras, and J. I. Cirac, Phys. Rev. Lett. **93**, 227205 (2004).
 - [6] N. Schuch, D. Pérez-García, and I. Cirac, Phys. Rev. B **84**, 165139 (2011).
 - [7] S. Sorella, S. Baroni, R. Car, and M. Parrinello, Europhysics Letters (EPL) **8**, 663 (1989).
 - [8] J. F. Corney and P. D. Drummond, Phys. Rev. Lett. **93**, 260401 (2004).
 - [9] K. B. Efetov, C. Pépin, and H. Meier, Phys. Rev. Lett. **103**, 186403 (2009).
 - [10] G. Carleo and M. Troyer, Science **355**, 602 (2017), <https://science.sciencemag.org/content/355/6325/602.full.pdf>.
 - [11] G. Carleo, I. Cirac, K. Cranmer, L. Daudet, M. Schuld, N. Tishby, L. Vogt-Maranto, and L. Zdeborová, Rev. Mod. Phys. **91**, 045002 (2019).
 - [12] G. Ausiello, P. Crescenzi, G. Gambosi, V. Kann, A. Marchetti-Spaccamela, and P. M.,
 - [13] B.-X. Zheng, C.-M. Chung, P. Corboz, G. Ehlers, M.-P. Qin, R. M. Noack, H. Shi, S. R. White, S. Zhang, and G. K.-L. Chan, Science **358**, 1155 (2017), <https://science.sciencemag.org/content/358/6367/1155.full.pdf>.
 - [14] S. Sorella, G. B. Martins, F. Becca, C. Gazza, L. Capriotti, A. Parola, and E. Dagotto, Phys. Rev. Lett. **88**, 117002 (2002).
 - [15] Considering the same unit the order parameter was consistent with the previous calculation obtained by VMC[14] at around 15% doping.
 - [16] F. Becca and S. Sorella, *Quantum Monte Carlo approaches for correlated systems* (Cambridge University Press, 2017).
 - [17] D. Eichenberger and D. Baeriswyl, Phys. Rev. B **76**, 180504 (2007).
 - [18] T. Yanagisawa, S. Koike, and K. Yamaji, Journal of the Physical Society of Japan **67**, 3867 (1998), <https://doi.org/10.1143/JPSJ.67.3867>.
 - [19] T. Yanagisawa, Journal of the Physical Society of Japan **85**, 114707 (2016), <https://doi.org/10.7566/JPSJ.85.114707>.
 - [20] M. J. S. Beach, R. G. Melko, T. Grover, and T. H. Hsieh, Phys. Rev. B **100**, 094434 (2019).
 - [21] D. Wecker, M. B. Hastings, and M. Troyer, Phys. Rev. A **92**, 042303 (2015).
 - [22] S. Sorella, Phys. Rev. Lett. **80**, 4558 (1998).
 - [23] S. Amari, Neural Computation **10**, 251 (1998).
 - [24] K. Seki and S. Sorella, Phys. Rev. B **99**, 144407 (2019).

- [25] D. S. Fisher, Phys. Rev. B **39**, 11783 (1989).
- [26] C. Lin, F. H. Zong, and D. M. Ceperley, Phys. Rev. E **64**, 016702 (2001).
- [27] C. Gros, Phys. Rev. B **53**, 6865 (1996).
- [28] S. Karakuzu, K. Seki, and S. Sorella, Phys. Rev. B **98**, 075156 (2018).
- [29] The numerator and the denominator of Eq. (11) are both real after summations over σ and σ' because they correspond to the RHS of Eq. (7) and the Hamiltonian is Hermitian. Therefore the real part \Re can be moved inside the summations of Eq. (11) with no approximation.
- [30] A. Griewank, *Evaluating Derivatives: Principles and Techniques of Algorithmic Differentiation* (Frontiers in Applied Mathematics, Philadelphia, 2000).
- [31] A. Griewank, Documenta Math. **Extra Volume**, 389 (2012).
- [32] S. Sorella and L. Capriotti, The Journal of Chemical Physics **133**, 234111 (2010), <https://doi.org/10.1063/1.3516208>.
- [33] H.-J. Liao, J.-G. Liu, L. Wang, and T. Xiang, Phys. Rev. X **9**, 031041 (2019).
- [34] L. F. Tocchio, A. Montorsi, and F. Becca, SciPost Phys. **7**, 21 (2019).
- [35] E. H. Lieb and F. Y. Wu, Phys. Rev. Lett. **20**, 1445 (1968).
- [36] V. J. Emery, S. A. Kivelson, and H. Q. Lin, Phys. Rev. Lett. **64**, 475 (1990).
- [37] J. P. F. LeBlanc, A. E. Antipov, F. Becca, I. W. Bulik, G. K.-L. Chan, C.-M. Chung, Y. Deng, M. Ferrero, T. M. Henderson, C. A. Jiménez-Hoyos, E. Kozik, X.-W. Liu, A. J. Millis, N. V. Prokof'ev, M. Qin, G. E. Scuseria, H. Shi, B. V. Svistunov, L. F. Tocchio, I. S. Tupitsyn, S. R. White, S. Zhang, B.-X. Zheng, Z. Zhu, and E. Gull (Simons Collaboration on the Many-Electron Problem), Phys. Rev. X **5**, 041041 (2015).
- [38] R. Hlubina, Phys. Rev. B **59**, 9600 (1999).
- [39] Y. Deng, E. Kozik, N. V. Prokofev, and B. V. Svistunov, EPL (Europhysics Letters) **110**, 57001 (2015).
- [40] C.-C. Chang and S. Zhang, Phys. Rev. B **78**, 165101 (2008).
- [41] S. Sorella, Phys. Rev. B **91**, 241116 (2015).